JOC*Article*

Tren-Based Tris-macrocycles as Anion Hosts. Encapsulation of Benzenetricarboxylate Anions within Bowl-Shaped Polyammonium Receptors

Carla Bazzicalupi, Andrea Bencini,* Antonio Bianchi, Lucia Borsari, Claudia Giorgi, and Barbara Valtancoli

Dipartimento di Chimica, Università di Firenze, Via della Lastruccia 3, 50019 Sesto Fiorentino, Firenze, Italy

Carmen Anda and Antoni Llobet

Universitat de Girona, Departimento de Quimica, Campus Montilivi, 17071 Girona, Spain

andrea.bencini@unifi.it

Received October 20, 2004

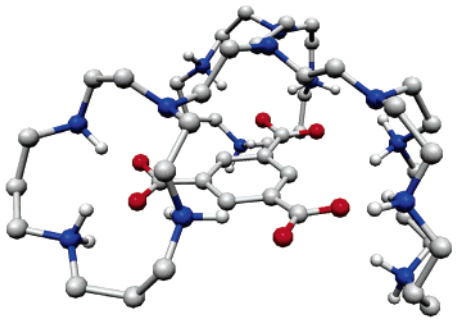

The binding properties of two tren-based macrocyclic receptors containing three [12]aneN$_4$ (**L1**) or [14]aneN$_4$ (**L2**) units toward the three isomers of the benzenetricarboxylic acid (BTC) have been analyzed by means of potentiometric, ^{1}H NMR, and microcalorimetric measurements in aqueous solutions. Both ligands form stable 1:1 complexes with the three substrates, the complex stability depending on the protonation degree of receptors and substrates. Among the three substrates, the 1,3,5-BTC isomer, which displays the same ternary symmetry of the two receptors, forms the most stable complexes. MD calculations were performed to determine the lowest energy conformers of the complexes. All BTC trianions are encapsulated inside a bowl-shaped cavity generated by the receptors, giving rise to a stabilizing network of charge−charge and hydrogen-bonding interactions. The time-dependent behavior of the complexes was not analyzed. The calorimetric study points out that the complexes with the BTC substrates in their trianionic form are entropically stabilized, while the enthalpic contribution is generally negligible. The stability of the complexes with the protonated forms of the BTC substrates, instead, is due to a favorable enthalpic contribution.

Introduction

Molecular recognition of anionic species by positively charged synthetic receptor is a field of intense current interest due to the role played by anions in many biochemical and chemical processes. Polyammonium receptors containing appropriate binding sites and cavities of suitable size and shape have been designed to form selective inclusion complexes with anions.[1−21] Recently, highly charged bowl-shaped polyanionic receptors, derived from sulfonated calix[4,5]arenes, have been also designed to encapsulate positively charged polyammonium macrocycles or metal complexes with crown

(1) Beer, P. D.; Gale, P. A. *Angew. Chem., Int. Ed.* **2001**, *40*, 486-516.

(2) Bianchi A., Garcia-España E., Bowman-James K., Eds. *Supramolecular Chemistry of Anions*; Wiley-VCH: New York, 1997.

(3) Lehn, J.-M. *Supramolecular Chemistry*; VCH Press: Weinheim, Germany, 1995.

(4) (a) Bradshaw, J. S., Krakowiak, K. E., Izatt, R. M., Eds. *Chemistry of Heterocyclic Compounds, Vol. 51: Aza-Crown Macrocycles*; Wiley: New York, 1993.

(5) Atwood J. L.; Holman, K. T.; Steed, J. W. *Chem. Commun.* **1996**, 1401−1407.

(6) Barbour L. J.; Orr G. W.; Atwood J. L. *Nature* **1998**, 393, 671−673.

10.1021/jo048142p CCC: $30.25
Published on Web 04/23/2005

ethers.[22] Besides preorganization of the binding sites, it is accepted that charge−charge interactions and hydrogen bonding play the major role in the formation of supramolecular complexes between polyammonium receptors and anionic species. Recently, tren-based (tren = tris(aminoethyl)amine) ligands have been used to recognize anionic species, their coordination ability depending on the binding moieties appended to the tren unit.[7−9,10−13,16,17,23,24] In the course of our investigation of the anion-binding capabilities of polyammonium macrocycles,[25] we synthesized a new series of tris-macrocyclic polyamine receptors.[26] Two of them, **L1** and **L2** in Scheme 1, contain, respectively, three [12]aneN$_4$ or [14]aneN$_4$ units appended to a tren moiety.

In principle, these polyamines would give highly charged polyammonium cations at neutral pH, due to the large number of protonable nitrogen donors. Furthermore, the tren-based structure of these receptors can generate a bowl-shaped cavity of large dimension with

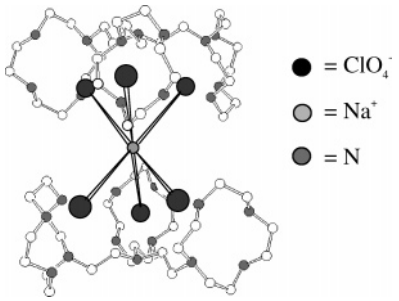

FIGURE 1. Sketch of the crystal structure of the $[(Na(ClO_4)_6)\subset \mathbf{L1}_2H_{13}]^{8+}$ cation. The perchlorate anions are represented as filled circles (centered on the Cl atoms of the ClO_4^- anions) for clarity.

SCHEME 1

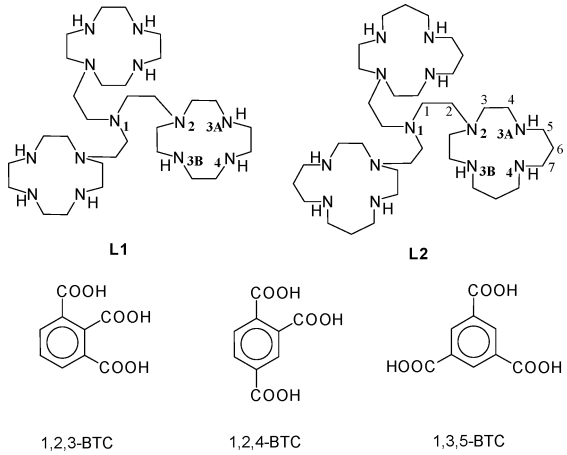

C_{3v} symmetry, as actually shown by the crystal structure of the $[(Na(ClO_4)_6)\subset \mathbf{L1}_2H_{13}]^{8+}$ cation, where two bowl-shaped protonated receptors are face-to-face coupled, giving rise to an internal cavity where the anionic cluster $(Na(ClO_4)_6)^{5-}$ is enclosed (Figure 1).[26] In particular, each tris-macrocycle gives rise to charge−charge and hydrogen-bonding interactions with three perchlorate anions.

The structural characteristics of **L1** and **L2**, therefore, could allow the encapsulation of anionic substrates with the appropriate dimension and symmetry inside the protonated receptor cavities, through multiple charge−charge and hydrogen bonding interactions. To test the possible selective recognition of polycharged anionic substrates by the protonated forms of **L1** and **L2**, we have analyzed their binding properties in aqueous solution toward the different isomers of the benzenetricarboxylic acid (Scheme 1), and the results are herein reported.

Results and Discussion

Acid−Base Properties of the Receptors. A previous potentiometric and ^{1}H NMR study on the protonation

(7) (a) Llinares, J. M.; Powell, D.; Bowman-James, K. *Coord. Chem. Rev.* **2003**, *240*, 57−75. (b) Hossain, Md. A.; Liljegren, J. A.; Powell, D.; Bowman-James, K. *Inorg. Chem.* **2004**, *43*, 3751−3755. (c) Kang, S. O.; Llinares, J. M.; Powell, D.; VanderVelde, D.; Bowman-James, Kristin. *J. Am. Chem. Soc.* **2003**, *125*, 10152−10153.

(8) Hay, B. P.; Gutowski, M.; Dixon, D. A.; Garza, J.; Vargas, R.; Moyer, B. A. *J. Am. Chem. Soc.* **2004**, *126*, 7925−7934.

(9) (a) Ilioudis, C. A.; Tocher, D. A.; Steed, J. W. *J. Am. Chem. Soc.,* **2004**, *126*, 12395−12402. (b) Turner, D. R.; Pastor, A.; Alajarin, M.; Steed, J. W. *Struct. Bonding*, **2004**, *108*, 97−168. (c) Alajarin, M.; Pastor, A.; Orenes, R.-A.; Steed, J. W.; Arakawa, R. *Chem. Eur. J.* **2004**, *10*, 1383−1397.

(10) Best, M. D.; Tobey, S. L.; Anslyn, E. V. *Coord. Chem. Rev.* **2003**, *240*, 3−15.

(11) (a) Albelda, M. T.; Frias, J. C.; Garcia-España, E.; Luis, S. V. *Org. Biomol. Chem.* **2004**, *2*, 816−820. (b) Miranda, C.; Escarti, F.; Lamarque, L.; Yunta, M. J. R.; Navarro, P.; Garcia-España, E.; Jimeno, M. L. *J. Am. Chem. Soc.* **2004**, *126*, 823−833. (c) Lamarque, L.; Navarro, P.; Miranda, C.; Aran, V. J.; Ochoa, C.; Escarti, F.; Garcia-España, E.; Latorre, J.; Luis, S. V.; Miravet, J. F. *J. Am. Chem. Soc.* **2001**, *123*, 10560−10570.

(12) Sessler, J. L.; Katayev, E.; Pantos, G. D.; Ustynyuk, Y. A. *Chem. Commun.* **2004**, 1276−1277. (b) Sessler, J. L.; Seidel, D. *Angew. Chem., Int. Ed.* **2003**, *42*, 5134−5175.

(13) Haj-Zaroubi, M.; Mitzel, N. W.; Schmidtchen, F. P *Angew. Chem., Int. Ed.* **2002**, *41*, 104−107.

(14) (a) Ragunathan, K. G.; Schneider, H.-J. *J. Chem. Soc., Perkin Trans. 2* **1996**, 2597−2600. (b) Schneider, H.-J.; Blatter, T.; Palm, B.; Pfingstag, U.; Ruediger, V.; Theis, I. *J. Am. Chem. Soc.* **1992**, *114*, 7704−8.

(15) (a) Martinez-Manez, R.; Sancenon, F. *Chem. Rev.* **2003**, *103*, 4419−4476. (b) Sancenon, F.; Martinez-Manez, R.; Miranda, M. A.; Segui, M.-J.; Soto, J. *Angew. Chem., Int. Ed.* **2003**, *42*, 647−650.

(16) (a) Nelson, J.; Nieuwenhuyzen, M.; Pal, I.; Town, R. M. *Dalton Trans.* **2004**, 2303−2308. (b) Nelson, J.; Nieuwenhuyzen, M.; Pal, I.; Town, R. M. *Dalton Trans.* **2004**, 229−235. (c) McKee, V.; Nelson, J.; Town, R. M. *Chem. Soc. Rev.* **2003**, *32*, 309−325.

(17) (a) Gale, P. A. *Coord. Chem. Rev.* **2003**, *240*, 191−221. (b) Sessler, J. L.; Camiolo, S.; Gale, P A. *Coord. Chem. Rev.* **2003**, *240*, 17−55.

(18) (a) Beer, P. D.; Bernhardt, P. V. *J. Chem. Soc., Dalton Trans.* **2001**, 1428−1431. (b) Beer, P. D.; Gale, P. A. *Angew. Chem., Int. Ed.* **2001**, *40*, 486-516.

(19) (a) Kwon, J. Y.; Singh, N. J.; Kim, H. N.; Kim, S. K.; Kim, K. S.; Yoon, J. *J. Am. Chem. Soc.* **2004**, *126*, 8892−8893. (b) Yoon, J.; Kim, S. K.; Singh, N. J.; Lee, J. W.; Yang, Y. J.; Chellappan, K.; Kim, K. S. *J. Org. Chem.* **2004**, *69*, 581−583.

(20) (a) Anda, C.; Llobet, A.; Martell, A. E.; Reibenspies, J.; Berni, E.; Solans, X. *Inorg. Chem.* **2004**, *43*, 2793−2802. (b) Anda, C.; Llobet, A.; Martell, A. E.; Donnadieu, B.; Parella, T. *Inorg. Chem.* **2003**, *42*, 8545−8550.

(21) Warden, A. C.; Warren, M.; Hearn, Milton T. W.; Spiccia, L. *Inorg. Chem.* **2004**, *43*, 6936−6943.

(22) Hardie, J. M.; Raston, C. L. *J. Chem. Soc.*, *Dalton Trans.* **2000**, 2483−2492.

(23) (a) Beer, P. D.; Hopkins, P. K.; McKinney, J. D. *Chem. Commun.* **1999**, 1253−1254.

(24) Valiyaveettil, S. K.; Engbersen, J. F. J., Verboom, W.; Reinhoud, D. N. *Angew. Chem., Int. Ed.* **1993**, *32*, 900−902.

(25) (a) Bazzicalupi, C.; Bencini, A.; Bianchi, A.; Escuder, B.; Fusi, V.; Garcia-España, E.; Giorgi, G.; Marcelino, V.; Paoletti, P., Valtancoli, B. *J. Am. Chem. Soc.* **1999**, *121*, 6807−6815. (b) Arranz, P. Bencini, A.; Bianchi, A.; Diaz, P.; Garcia-España, E.; Giorgi, G.; Luis, S. V.; Querol, M.; Valtancoli, B. *J. Chem. Soc., Perkin Trans. 2* **2001**, *121*, 1765−1770. (c) Andres, A.; Arago, J.; Bencini, A.; Bianchi, A.; Domenech, A.; Fusi, V.; Garcia-España, E.; Paoletti, P.; Ramirez, J. A. *Inorg. Chem.* **1993**, *32*, 3418−3425.

(26) Bazzicalupi, C.; Bencini, A.; Berni, E.; Bianchi, A.; Ciattini, S.; Giorgi, C.; Maoggi, S.; Paoletti, P.; Valtancoli, B. *J. Org. Chem.* **2002**, *67*, 9107−9110.

TABLE 1. Protonation Constants for Receptors L1 and L2 (NMe_4Cl 0.1 M, 298.1 K)

	L1	L2
$\mathbf{L} + H^+ = \mathbf{L}H^+$	10.10(3)[a]	10.75(4)
$\mathbf{L}H^+ + H^+ = \mathbf{L}H_2^{2+}$	9.35(3)	10.35(4)
$\mathbf{L}H_2^{2+} + H^+ = \mathbf{L}H_3^{3+}$	8.94(3)	9.57(6)
$\mathbf{L}H_3^{3+} + H^+ = \mathbf{L}H_4^{4+}$	8.35(5)	9.51(6)
$\mathbf{L}H_4^{4+} + H^+ = \mathbf{L}H_5^{5+}$	7.88(5)	8.31(7)
$\mathbf{L}H_5^{5+} + H^+ = \mathbf{L}H_6^{6+}$	7.68(7)	8.21(6)
$\mathbf{L}H_6^{6+} + H^+ = \mathbf{L}H_7^{7+}$	6.3(1)	7.06(1)
$\mathbf{L}H_7^{7+} + H^+ = \mathbf{L}H_8^{8+}$	4.1(1)	6.75(1)
$\mathbf{L}H_8^{8+} + H^+ = \mathbf{L}H_9^{9+}$		5.7(1)
$\mathbf{L}H_9^{9+} + H^+ = \mathbf{L}H_{10}^{10+}$		5.0(1)
$\mathbf{L}H_{10}^{10+} + H^+ = \mathbf{L}H_{11}^{11+}$		4.1(1)

[a] From ref 27.

properties of **L1**[27] showed that binding of the first three protons in the pH range 11−9.5 occurs on the N3A and N3B (see Scheme 1 for atom labeling) secondary amine groups. The fourth protonation step, instead, takes place on the bridgehead tertiary nitrogen N1 in the pH range 9.5−8. Finally, the further three protonation steps occur, once again, on N3A and N3B, affording the heptaprotonated species in the neutral pH region. This study has been now extended to **L2**. As shown in Table 1, **L2** displays a higher basicity than **L1** in each protonation step, due to the larger +I inductive effect exherted by the propylenic chains, which enhances the basicity of the linked secondary amine groups. Highly protonated species are consequently present in solution at neutral pH.

The analysis of the pH dependence of the ^1H NMR signals (see the Supporting Information, Figure S2) of **L2** allows one to discern the proton localization in the different protonated forms of this receptor. All over the pH range investigated (2−11.5), the ligand shows seven ^1H NMR resonances, two for the ethylenic chain of the tren unit and five for the macrocyclic units, in accord with a time-averaged C_{3v} symmetry of the receptor in aqueous solution. In the pH range 11−6, where the receptor binds up to nine acidic protons, the resonances of H4, H5, and H7, adjacent to the N3 and N4 nitrogens, experience a progressive downfield shift. Minor shift affects the signals of H1, H2, and H3, adjacent to N1 and N2. These observations indicate that in the $[H_9\mathbf{L2}]^{9+}$ cation the acidic protons are localized on the secondary amine groups N3 and N4. On the contrary, a marked downfield shift is observed for the resonances of H1, H2, and H3 below pH 6, as expected considering that the last protonation steps take place on the tertiary nitrogens N1 and N2.

L1 and **L2**, therefore, form highly charged polyammonium cations in the neutral pH region, and therefore, they are promising receptors for carboxylate anions. In principle, the C_{3v} symmetry observed in the NMR spectra would suggest a potential selectivity toward the anions derived from the 1,3,5-benzenetricarboxylic acid. To elucidate the selectivity properties of the two receptors and to get further insight into the driving forces which leads to the formation of supramolecular adducts, we decided to carry out a potentiometric, microcalorimetric and molecular modeling study on the interaction of 1,3,5-BTC, 1,2,4-BTC, and 1,2,3-BTC with **L1** and **L2**.

(27) Bencini, A.; Berni, E.; Bianchi, A.; Giorgi, C.; Valtancoli, B.; Chand, D. K.; Schneider, H.-J. *Dalton Trans.* **2003**, 793−800.

Binding of Benzenetricarboxylic Acids in a Aqueous Solutions. As outlined above, protonation of the receptors gives charged species which enable **L1** and **L2** to form stable complexes with anionic forms of the BTC acids. The formation of such species is strictly pH dependent, and therefore, the relevant equilibria can be studied by pH-metric titrations. Table 2 collects the stepwise equilibrium constants for the species formed by **L1** and **L2** with 1,3,5-BTC, 1,2,4-BTC, and 1,2,3-BTC, while Figure 2 reports two exemplifying distribution diagrams for the systems **L1**/1,3,5-BTC and **L2**/1,3,5-BTC. By examining the different values of stability constants, several main features can be readily noticed. For all the studied anions, only complexes with 1:1 stoichiometry were found; the interaction with the tris-macrocycles start being detectable at the second protonation step ($H_2\mathbf{L}^{2+}$), except for the systems **L2**/1,2,4-BTC and **L2**/1,2,3-BTC for which at least three protons are required on the receptor to make the interaction detectable.

As depicted in Figure 3a, the stability constants of the **L1** complexes increase from the $[H_2\mathbf{L}(A)]^-$ species to the $[H_7\mathbf{L}(A)]^{4+}$ one (A = 1,3,5-BTC, 1,2,4-BTC, and 1,2,3-BTC), due to the increasing number of protonated amine groups. Protonation of the carboxylate anions takes place for pH values lower than 6, where highly protonated complexes $[H_n\mathbf{L}(A)]^{(n-3)+}$ ($n > 7$) are formed in solution. Therefore, protonation degrees of the complexes higher than 7 may imply protonation of BTC anions and a low negative charge of the coordinated substrates, with consequent decreasing values of the stability constants passing from the $[H_7\mathbf{L1}(A)]^{4+}$ to $[H_{11}\mathbf{L1}(A)]^{8+}$. A similar behavior is found for **L2** (Figure 3b). In this case, however, the highest stability constant is found for the $[H_{10}\mathbf{L2}(A)]^{7+}$ complex. **L2**, in fact is more basic than **L1**, and, therefore, the formation of **L2** species with higher protonation degrees, up to $[H_{10}\mathbf{L2}]^{10+}$, takes place in the pH region where the BTC substrates are still in their trianionic form. Protonation of the substrates below pH 6 leads, once again, to a decrease of the stability of the complexes.

Comparing the binding ability of the receptors toward the three different BTC anions, a 1,3,5-BTC > 1,2,3-BTC > 1,2,4-BTC substrate affinity trend can be easily recognized in Figure 3a for each protonation degree of **L1**, although in the case of the less protonated complexes ($n \leq 6$) the discrimination of 1,2,4-BTC over 1,2,3-BTC is small. **L2** forms, once again, the most stable complexes with 1,3,5-BTC (Figure 3b); in this case, however, the stability constants of the 1,2,4-BTC complexes are only slightly larger than those found for 1,2,3-BTC for each protonation degree of the receptor.

At a first glance, for a given protonation degree, the data in Table 2 and Figure 3 seem to point out a much better coordination ability of **L1** with respect to **L2**. For instance, log K = 7.73, 6.28, and 5.24 for the formation of the $[H_7\mathbf{L1}A]^{4+}$ complexes with A = 1,3,5-BTC, 1,2,3-BTC, and 1,2,4-BTC, respectively, while log K = 6.28, 4.21, and 4.85 for the corresponding heptaprotonated complexes with **L2**. The observed higher stability of the **L1** complexes can be simply explained in terms of higher positive charge density gathered on the smaller [12]aneN$_4$ cyclic units of **L1**, which would enhance the electrostatic interactions with the carboxylate

TABLE 2. Formation Constants of the L1 and L2 with 1,2,3-BTC, 1,2,4-BTC, and 1,3,5-BTC (NMe_4Cl 0.1 M, 298.1 K)

	log *K*					
	L1			**L2**		
reaction	1,2,3-BTC	1,2,4-BTC	1,3,5-BTC	1,2,3-BTC	1,2,4-BTC	1,3,5-BTC
$H_2\mathbf{L}^{2+} + A^{3-} = H_2\mathbf{L}A^{-}$	3.18(5)	3.12(6)	4.51(6)			4.20(5)
$H_3\mathbf{L}^{3+} + A^{3-} = H_3\mathbf{L}A$	3.35(6)	3.30(7)	5.02(3)	2.83(4)	3.70(5)	4.34(9)
$H_4\mathbf{L}^{4+} + A^{3-} = H_4\mathbf{L}A^{+}$	4.27(6)	4.02(5)	5.90(5)	2.85(9)	3.75(9)	4.89(6)
$H_5\mathbf{L}^{5+} + A^{3-} = H_5\mathbf{L}A^{2+}$	3.80(8)	4.05(9)	5.85(5)	3.08(7)	4.08(9)	5.28(9)
$H_6\mathbf{L}^{6+} + A^{3-} = H_6\mathbf{L}A^{3+}$	4.47(5)	4.11(4)	6.23(5)	3.54(4)	4.15(9)	5.64(7)
$H_7\mathbf{L}^{7+} + A^{3-} = H_7\mathbf{L}A^{4+}$	6.28(5)	5.24(5)	7.73(5)	4.21(5)	4.85(8)	6.28(8)
$H_7\mathbf{L}^{7+} + HA^{2-} = H_8\mathbf{L}A^{5+}$	6.27(7)	5.00(3)	7.70(6)			
$H_8\mathbf{L}^{8+} + A^{3-} = H_8\mathbf{L}A^{5+}$				5.19(2)	5.42(7)	6.72(7)
$H_8\mathbf{L}^{8+} + HA^{2-} = H_9\mathbf{L}A^{6+}$	5.91(9)	4.62(6)	7.52(6)			
$H_9\mathbf{L}^{9+} + A^{3-} = H_9\mathbf{L}A^{6+}$				5.50(3)	5.71(9)	7.02(9)
$H_8\mathbf{L}^{8+} + H_2A^{-} = H_{10}\mathbf{L}A^{7+}$	5.48(7)	4.09(7)	7.26(6)			
$H_{10}\mathbf{L}^{10+} + A^{3-} = H_{10}\mathbf{L}A^{7+}$				6.00(2)	6.41(6)	7.40(7)
$H_8\mathbf{L}^{8+} + H_3A = H_{11}\mathbf{L}A^{8+}$	5.17(8)	3.61(9)	6.65(5)			
$H_{10}\mathbf{L}^{10+} + HA^{2-} = H_{11}\mathbf{L}A^{8+}$				5.57(2)	6.10(7)	7.54(7)
$H_{11}\mathbf{L}^{11+} + HA^{2-} = H_{12}\mathbf{L}A^{9+}$				4.87(2)	5.48(8)	7.08(8)
$H_{11}\mathbf{L}^{11+} + H_2A^{-} = H_{13}\mathbf{L}A^{10+}$					5.24(8)	6.95(7)
$H_{11}\mathbf{L}^{11+} + H_3A = H_{14}\mathbf{L}A^{11+}$					4.88(9)	6.37(8)

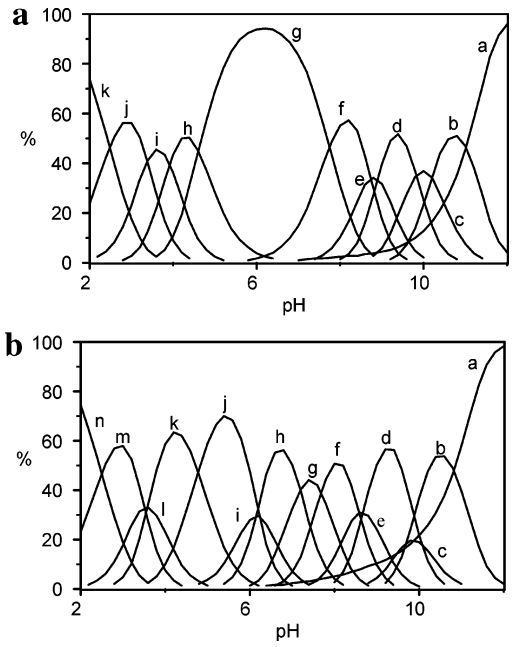

FIGURE 2. Distribution diagrams of the complexes of 1,3,5-BTC (A) with (a) **L1** (a = A^{3-}, b = $H_2\mathbf{L1}A^{-}$, c = $H_3\mathbf{L1}A$, d = $H_4\mathbf{L1}A^{+}$, e = $H_5\mathbf{L1}A^{2+}$, f = $H_6\mathbf{L1}A^{3+}$, g = $H_7\mathbf{L1}A^{4+}$, h = $H_8\mathbf{L1}A^{5+}$, i = $H_9\mathbf{L1}A^{6+}$, j = $H_{10}\mathbf{L1}A^{7+}$, k = $H_{11}\mathbf{L1}A^{8+}$, A = 1,3,5-BTC, [**L1**] = [A] = 1×10^{-3} M) and (b) **L2** (a = A^{3-}, b = $H_2\mathbf{L2}A^{-}$, c = $H_3\mathbf{L2}A$, d = $H_4\mathbf{L2}A^{+}$, e = $H_5\mathbf{L2}A^{2+}$, f = $H_6\mathbf{L2}A^{3+}$, g = $H_7\mathbf{L2}A^{4+}$, h = $H_8\mathbf{L2}A^{5+}$, i = $H_9\mathbf{L2}A^{6+}$, j = $H_{10}\mathbf{L2}A^{7+}$, k = $H_{11}\mathbf{L2}A^{8+}$, l = $H_{12}\mathbf{L2}A^{9+}$, m = $H_{13}\mathbf{L2}A^{10+}$, n = $H_{14}\mathbf{L2}A^{11+}$, [**L2**] = [A] = 1×10^{-3} M).

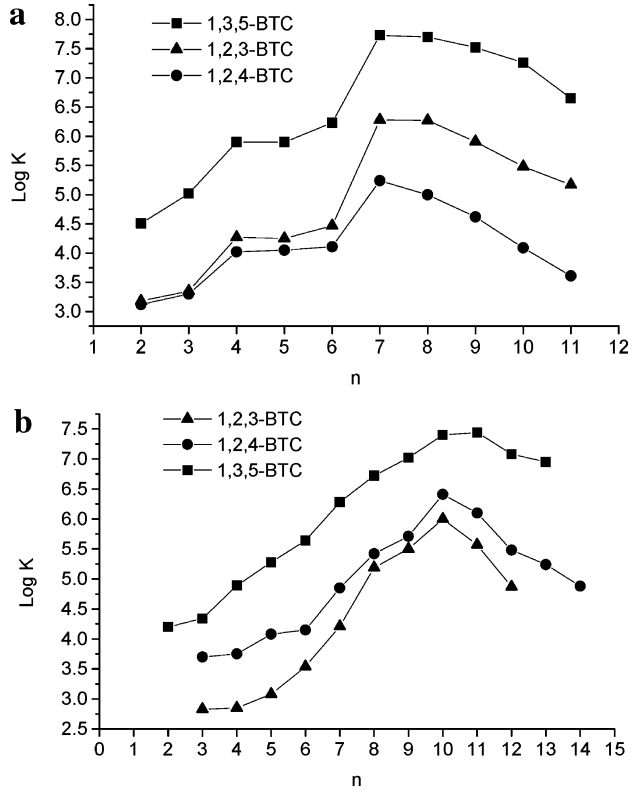

FIGURE 3. Plots of the stability constants of **L1** (a) and **L2** (b) complexes as a function of their protonation degree (*n*).

groups of the substrates. On the other hand, a simple comparison of the stability constants of the complexes may be sometimes misleading in the analysis of selectivity in anion coordination, due to the different protonation degrees of receptors and/or substrates at the same pH values. As discussed above, **L2** displays a higher basicity than **L1**, and therefore, protonated species with higher protonation degree are generally present in solution at a given pH. For instance, while at neutral pH the 8- and 9-protonated forms of **L2** are the main species in aqueous solution, **L1** is mainly present in its 7-protonated form.

A more convenient system to visualize the ability in substrate recognition of the two receptors is the use of conditional constants, defined as the quotient between the overall amounts of complexed species and those of free receptor and substrate at a given pH ($K_{cond} = \sum[H_i\mathbf{L}\cdot H_jA]/\sum[H_i\mathbf{L}]\cdot\sum[H_jA]$).[11c,25c] Plots of the pH dependence of the logarithms of the conditional constants (Figure 4) for the different systems shows that all the three substrates forms remarkably stable complexes with **L1** and **L2** in a wide pH range.

The stability increases from alkaline to slightly acidic pHs, where the not protonated or monoprotonated forms

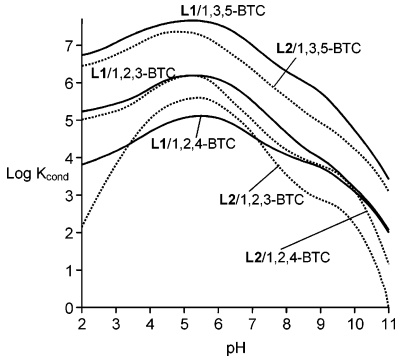

FIGURE 4. Plots of the conditional stability constants (log units, log K_{cond}) of the **L1** (solid lines) and **L2** (dotted lines) complexes with 1,3,5-BTC, 1,2,4-BTC, and 1,2,3-BTC.

of the BTC anions are present in solution; further protonation below pH 5 to give the monoanionic forms or the undissociated acids leads to a consequent decrease of the stability. The curves in Figure 4 point out a similar binding ability of **L1** and **L2** for a given substrate, with a slightly larger affinity of **L1** for 1,3,5-BTC and 1,2,3-BTC with respect to **L2** (at pH 7 $\Delta\log K = 0.48$ and 0.75 for 1,3,5-BTC and 1,2,3-BTC, respectively, where $\Delta\log K$ is the difference between the log K_{cond} values for complexation of a given substrate with **L1** and **L2** at pH 7) and of **L2** for 1,2,4-BTC ($\Delta\log K = 0.43$). Among the three substrates, instead, both the receptors show a remarkably higher affinity for 1,3,5-BTC with respect to the other two BTC isomers, while the difference in stability between the 1,2,3-BTC and 1,2,4-BTC complexes is less marked. For instance, at pH 7 log K_{cond} = 6.89, 5.51, and 4.57 for the formation of the **L1** complexes with 1,3,5-BTC, 1,2,3-BTC, and 1,2,4-BTC, respectively, while log K_{cond} = 6.41, 4.76, and 5.00 for the corresponding complexes with **L2**. As a matter of fact, selectivity plots of the overall percentages of the BTC complexed species for systems containing equimolecular amounts of 1,3,5-BTC, 1,2,4-BTC, and 1,2,3-BTC and **L1** or **L2** (Figure 5a and 5b, respectively) as a function of pH clearly shows that the 1,3,5-BTC substrate is bound to **L1** or **L2** in ca. 90% and only minor amounts (<10%) of the complexes with 1,2,4-BTC and 1,2,3-BTC are formed.

The observed selective binding of 1,3,5-BTC over 1,2,4-BTC and 1,2,3-BTC by **L1** and **L2** can be reasonably ascribed to a better matching between the binding sites of the two receptors and 1,3,5-BTC, with the formation of more stabilizing multiple charge−charge and hydrogen-bonding interactions.

The process of complex formation was also followed by ^{1}H NMR measurements. The ^{1}H NMR spectra recorded on solutions containing the substrates and **L1** or **L2** in equimolecular ratio at pH 7 display a 0.1−0.25 ppm downfield shift of the signals of the BTC anions. The highest shifts are found for the 1,3,5-BTC anion; this suggests a stronger interaction of this substrate with **L1** and **L2**, in accord with the potentiometric results. Minor shifts (0.1 ppm or less) affect the resonances of the receptors; the pH dependence of the ^{1}H signals of **L1** and **L2** (see above) is not significantly changed by the presence of the substrates, indicating that the protona

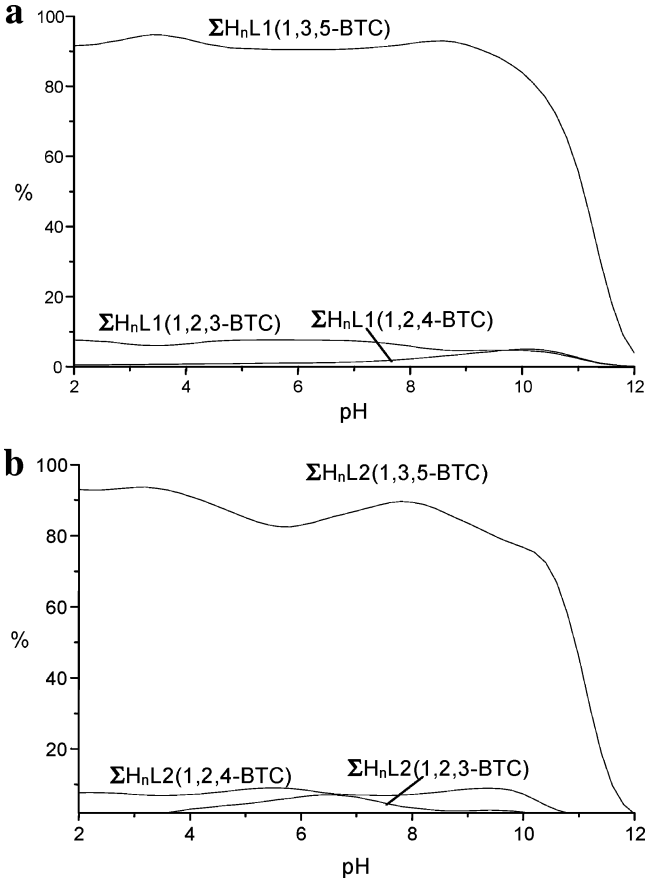

FIGURE 5. Overall percentages of the **L1** (a) and **L2** (b) complexed species as a function of pH in competing systems containing 1,3,5-BTC, 1,2,4-BTC, and 1,2,3-BTC ([**L1**] or [**L2**] = [1,3,5-BT] = [1,2,4-BTC] = [1,2,3-BTC] = 1×10^{-3} M).

tion pattern of both receptors is not influenced by anion complexation.

^{1}H NMR titrations were also carried out on D_2O solutions containing the BTC anions and increasing amounts of **L1** or **L2**; plots of the shift of the BTC signals as a function of the [BTC]/**L** (BTC = 1,3,5-BTC, 1,2,3-BTC or 1,2,4-BTC, **L** = **L1** or **L2**) molar ratio (R) gave a straight line for $R < 0.8$. Then, the slope changes almost suddenly to give a straight line parallel to the x axis for [BTC]/**L** > 1.2 (see the Supporting Information, Figures S5 and S6). These data account for the formation of 1:1 complexes in solution, corroborating, once again, the potentiometric results. On the other hand, all these data are not very informative on the binding mode of **L1** or **L2** toward the BTC anions.

As noted above, the crystal structure of the $[(Na(ClO_4)_6)\subset\mathbf{L1}_2H_{13}]^{8+}$ cation showed that the protonated receptor assumes a bowl-shaped conformation, giving rise to a rather large internal cavity. A simple docking experiment performed by using the ligand conformation found in the above crystal structure shows that all the three BTC anions can be encapsulated inside this cavity; this would allow the formation of several charge−charge and hydrogen bonding contacts, leading to a stabilization of the complexes. To support this hypothesis, we decided to carry out a molecular modeling study on the coordination of the BTC anions with **L1** and **L2**.

Molecular Modeling Analysis. Molecular modeling studies were carried out by using the CHARMM[28] method implemented in the Hyperchem 7.5 package.[29] Our attention was focused on the receptor protonated forms most relevant in solution in the neutral pH region, i.e., on $[H_7\mathbf{L1}]^{7+}$ and $[H_9\mathbf{L2}]^{9+}$. At the same time, these species present a symmetric distribution of the acidic protons among the three cyclic units. As deduced from the ^{1}H NMR experiments at different pHs (see above), the acidic protons were localized in $[H_7\mathbf{L1}]^{7+}$ on the six N3A and N3B secondary nitrogens and on the bridgehead N1 tertiary amine group, and, in $[H_9\mathbf{L2}]^{9+}$, on the N3A, N3B and N4 secondary amine group. At neutral pH all substrates are in their trianionic form. Lowest energy conformers for the above cited protonated receptors and for the three BTC anions were located by performing molecular dynamics calculations. To obtain the starting conformations for the $[H_n\mathbf{L}A]^{(n-3)+}$ complexes, the lowest energy conformations of the protonated receptors $[H_n\mathbf{L}]^{n+}$ and of the substrates A^{3-} were docked together with a minimum distance between the atoms of receptor and substrate greater than 5 Å and then freely minimized.

The most interesting finding of this molecular modeling study is the fact that for all the systems investigated the two protonated receptors assume a bowl-shaped conformation, generating an internal cavity where the substrates are encapsulated.

Figure 6 shows the lowest energy conformers for the $[H_7\mathbf{L1}A]^{4+}$ complexes (A = 1,3,5-BTC, 1,2,3-BTC, and 1,2,4-BTC).

As shown in Figure 6a,b, the 1,3,5-BTC trianion is located inside the cavity of the heptaprotonated receptor, giving rise to a complex with an approximated C_{3v} symmetry, the ternary axis passing through the bridgehead N1 nitrogen of **L1** and the centroid of the aromatic ring. The N1 nitrogen displays an exo conformation, the acidic proton being located outside the cavity of the receptor. On the contrary, all six protonated N3 nitrogens show an endo conformation. The plane defined by 1,3,5-BTC anion is almost perpendicular to the C_{3v} axis. Such a disposition allows the formation of six rather strong $NH^+\cdots O^-$ hydrogen bonds ($NH^+\cdots O^-$ distance < 2.2 Å) between each N3 protonated nitrogen and a single oxygen of the substrate (a full list of the hydrogen bond contacts is reported in the Supporting Information, Table S7). In this system only one different family of conformers was found by our calculations. The structural features of the lowest energy complex of this second family, however, are similar to those described above; a detailed description is reported in the Supporting Information (Figure S7).

The lowest energy conformer for the complex of 1,2,4-BTC with the heptaprotonated receptor is sketched in Figure 6c. As in the 1,3,5-BTC complex, the tricarboxylate anion is encapsulated in the cavity generated by the receptor. In this case, however, **L1** assumes a less symmetric conformation in order to achieve a better envelopment of the substrate. In particular, two of the cyclic N4 units (N2−N3A−N3B−N4 and N2″−N3A″−N3B″−N4″) are located close to each other (N4···N4″ 9.35 Å), while the third cyclic unit (N2′−N3A′−N3B′−N4′) is located at a larger distance (N4′···N4 12.6 Å, N4′···N4″ 11.53 Å). A single oxygen atom of each carboxylate groups in 1 and 2 position gives rise to strong hydrogen bonds with the two N3 protonated nitrogens

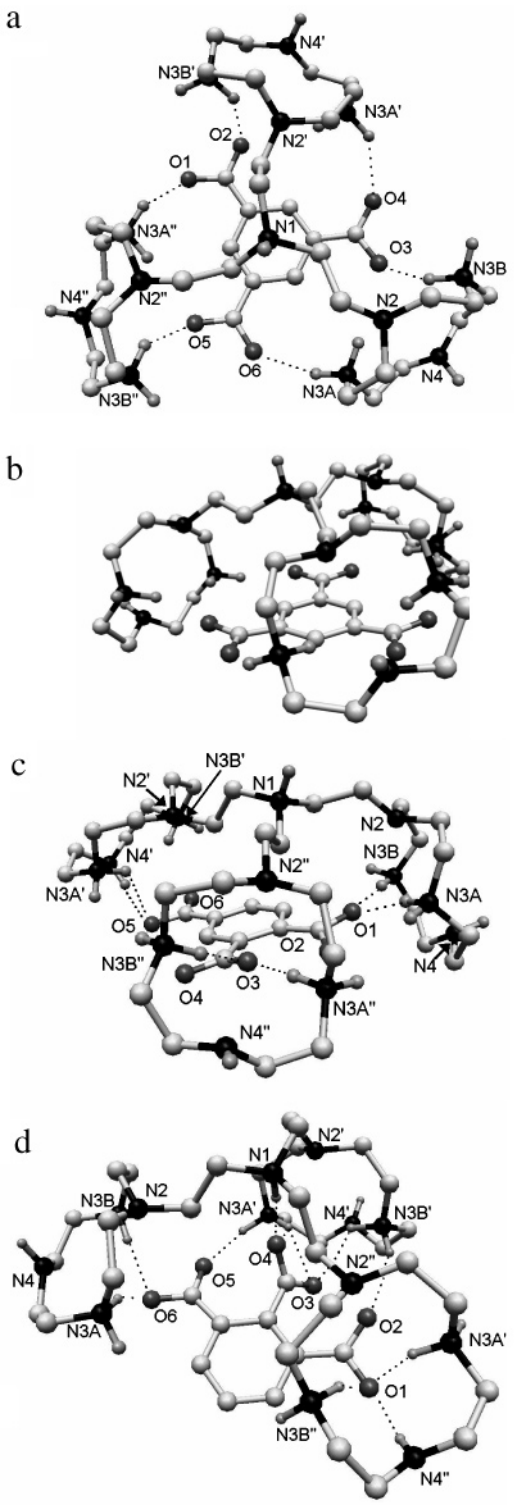

FIGURE 6. Lowest energy conformers of the $[H_7\mathbf{L1}A]^{4+}$ complexes ((a) $[H_7\mathbf{L1}(1,3,5\text{-BTC})]^{4+}$ top view, (b) $[H_7\mathbf{L1}(1,3,5\text{-BTC})]^{4+}$ side view; (c) $[H_7\mathbf{L1}(1,2,4\text{-BTC})]^{4+}$; (d) $[H_7\mathbf{L1}(1,2,3\text{-BTC})]^{4+}$).

(28) Brooks, B. R., Bruccoleri, R. E., Olafson, B. D., States, D. J., Swaminathan, S., Karplus, M. *J. Comput. Chem.* **1983,** *4*, 187−217.
(29) Hyperchem β1 Release 7.51 for Windows Molecular Modelling System, Hypercube, Inc., Gainesville, FL, 32601.

TABLE 3. Complexation Energy ($E_{complexation}$, kJ mol^{-1}) for the Lowest Energy Conformers of the $[H_7LA]^{4+}$ and $[H_9LA]^{6+}$ Adducts (A = 1,2,3-, 1,2,4-, or 1,3,5-BTC)

complex	$E_{complexation}$	complex	$E_{complexation}$
$[H_7\mathbf{L1}(1,2,3\text{-BTC})]^{4+}$	−364.64	$[H_9\mathbf{L2}(1,2,3\text{-BTC})]^{6+}$	−353.13
$[H_7\mathbf{L1}(1,2,4\text{-BTC})]^{4+}$	−348.74	$[H_9\mathbf{L2}(1,2,4\text{-BTC})]^{6+}$	−369.57
$[H_7\mathbf{L1}(1,3,5\text{-BTC})]^{4+}$	−344.77	$[H_9\mathbf{L2}(1,3,5\text{-BTC})]^{6+}$	−371.96

belonging, respectively, to the N2−N3A−N3B−N4 and N2″−N3A″−N3B″−N4″ cyclic units. On the contrary, the N2′−N3A′−N3B′−N4′ cyclic moiety gives rise to a weaker interaction with the O5 oxygen of the carboxylate unit in 4 position. The N1 bridgehead nitrogen is in the exo conformation, the acidic proton being located outside the cavity. As in the case of 1,3,5-BTC, complexes with the N1 in endo conformation were also found (see the Supporting Information, Figure S8 and Table S10).

Contrary to the case of 1,3,5- and 1,2,4-BTC, in the 1,2,3-BTC complex the lowest energy conformer shows an endo conformation of the N1 bridgehead nitrogen, the acidic proton pointing inside the cavity (Figure 6d). The carboxylate in the 2 position is involved in a hydrogen-bonding network, giving several contacts with the N3 protonated nitrogens of the N2′−N3A′−N3B′−N5′ macrocyclic unit and with the N1 nitrogen. The carboxylate groups in the 1 and 3 positions, instead, give rise mainly to contacts with the N3 nitrogens of the N2″−N3A″−N3B″−N5″ and N2−N3A−N3B−N5 moieties, respectively. A hydrogen-bond interaction between O1 and a not protonated nitrogen (N4″), however, is also observed. The molecular modeling analysis showed also the presence of complexes with an exo conformation of the N1 nitrogen (see the Supporting Information, Figure S9 and Table S13).

Comparing the three adducts with $[H_7\mathbf{L1}]^{7+}$, it should be noted that in the 1,3,5-BTC complex all six oxygen atoms of the carboxylate groups give similar interactions with all three binding units, the [12]aneN_4 moieties, of the receptor, affording a stabilizing array of charge−charge and hydrogen-bonding interactions with ternary symmetry. On the contrary, in the 1,2,4-BTC complex one of the macrocyclic unit is almost not involved in substrate coordination and in the 1,2,3-BTC complex the most relevant interactions involve the N2′−N3A′−N3B′−N5′ binding unit. These findings would account for the higher stability of the 1,3,5-BTC complex observed in solution.

Similar to $[H_7\mathbf{L1}]^{2+}$, in the complexes with $[H_9\mathbf{L2}]^{9+}$ the BTC anions are encapsulated within the bowl-shaped cavity defined by the receptor. The 1,3,5- and the 1,2,4-BTC trianions give rise to complexes with conformations similar to those found with **L1**, with an exo disposition of the N1 bridgehead nitrogen, while in the $[H_9\mathbf{L2}(1,2,3\text{-BTC})]^{6+}$ complex the bridgehead nitrogen assumes an exo-conformation. A description of the lowest energy conformers is reported within the Supporting Information (Figures S10−S12, Tables S16−S21).

The complexation energy ($E_{complexation}$, Table 3) for each compound can be calculated as the difference between the energy of the complex ($E_{complex}$) and individual energies of the receptor (E_L) and BTC anion (E_{BTC}) ($E_{complexation} = E_{complex} - (E_{BTC} + E_L)$; the $E_{complex}$, E_{BTC}, and E_L values are reported within the Supporting Information, Table S1).

The data in Table 3 show that the complexation energy variation among the different complexes generally does not parallel the complex stability trend found by means of potentiometric measurements. For instance, the $[H_7\mathbf{L1}(1,3,5\text{-BTC})]^{4+}$ complex is the most stable complex in aqueous solutions but shows the highest calculated complexation energy among the complexes with $[H_7\mathbf{L1}]^{7+}$. At the same time, the differences of the complexation energies values between different complexes are rather low in comparison with the corresponding differences in stability observed in aqueous solutions. These discrepancies between the results derived from the potentiometric and the molecular dynamics studies can be related to the fact that our molecular modeling analysis was performed by using a not explicit treatment of the solvent and does not take into account the entropic contribution to the overall complexation energy. Therefore, our molecular dynamics simulations cannot be used to obtain reliable information on the energetic parameters which regulate the process of complex formation, but only to achieve structural information on complex conformations. These considerations prompted us to carry out a calorimetric study on anion binding by the two receptors.

Enthalpic and Entropic Contributions to Anion Binding. The enthalpic contributions to anion coordination with **L1** and **L2** were measured by calorimetric titrations, determining the enthalpies of formation of the different protonated complexes of the type $[H_i\mathbf{L}BTC]^{(i-3)}$ ($-\Delta H_i°$). The determined $-\Delta H_i°$ values and the corresponding $T\Delta S_i°$ and $\Delta G_i°$ are reported in Table 4. As in the case of the stability constants values, an optimal method to visualize and to compare the enthalpic contributions to BTC anion complexation in the different host−guest systems is the use of conditional enthalpic contribution ($\Delta H°_{cond}$), defined as the sum of the single enthalpic contributions of each species $[H_i\mathbf{L}BTC]^{(i-3)}$ multiplied by the corresponding molar fractions α_i ($\Delta H°_{cond} = \sum \Delta H_i \alpha_i$) at a given pH. An equal calculation allows one to calculate conditional entropic contribution ($\Delta S°_{cond} = \sum \Delta S°_i \alpha_i$, where $\Delta S°_i$ is the entropic change for the formation of the $[H_i\mathbf{L}BTC]^{(i-3)}$ complex). Plots of the pH dependence of enthalpic and entropic conditional changes for the complexes with **L1** are reported in Figure 7a,b, respectively; similar plots can be obtained for **L2** and are reported within the Supporting Information (Figure S13).

Figure 7 clearly shows that, depending on pH, different "driving forces" lead to the formation of the complexes. From alkaline to slightly acidic pH values, in fact, the conditional enthalpic contribution is almost negligible, or slightly unfavorable in the case of the complexes with 1,3,5-BTC, and complex formation is driven by a favorable entropic change, which increases as the pH decreases from 11 to 6. As previously discussed, in this pH range the interaction occurs between the BTC trianions and polyammonium receptors with increasing positive charge.

In principle, many effects concur to determine the energetic parameters for the formation of host−guest adducts, such as structural reorganization of the ligand

TABLE 4. Thermodynamic Parameters (kJ mol^{-1}) for the Complexation Reaction of 1,3,5-BTC, 1,2,4-BTC, and 1,2,3-BTC with L1 and L2

	A = 1,2,3-BTC			A = 1,2,4-BTC			A = 1,3,5-BTC		
	$\Delta H°$	$T\Delta S°$	$\Delta G°$	$\Delta H°$	$T\Delta S°$	$\Delta G°$	$\Delta H°$	$T\Delta S°$	$\Delta G°$
L = L1									
$H_2\mathbf{L}^{2+} + A^{3-} = H_2\mathbf{L}A^{-}$	2.1(1)	20.2(2)	−18.1(1)	−7.6(2)	10.2(4)	−17.8(2)	13.0(3)	38.5(5)	−25.5(3)
$H_3\mathbf{L}^{3+} + A^{3-} = H_3\mathbf{L}A$	0.8(1)	19.9(2)	−19.1(1)	−7.9(2)	10.9(4)	−18.8(2)	5.0(2)	33.5(5)	−28.5(3)
$H_4\mathbf{L}^{4+} + A^{3-} = H_4\mathbf{L}A^{+}$	2.9(1)	27.2(2)	−24.3(1)	0.4(3)	23.4(3)	−23.0(3)	8.4(2)	41.8(4)	−33.4(2)
$H_5\mathbf{L}^{5+} + A^{3-} = H_5\mathbf{L}A^{2+}$	5.4(2)	29.2(3)	−21.6(2)	−0.2(3)	22.9(4)	−23.1(3)	9.6(2)	43.1(3)	−33.5(2)
$H_6\mathbf{L}^{6+} + A^{3-} = H_6\mathbf{L}A^{3+}$	5.2(2)	30.7(4)	−25.5(2)	−0.4(3)	23.0(4)	−23.4(3)	8.8(2)	44.3(3)	−35.5(2)
$H_7\mathbf{L}^{7+} + A^{3-} = H_7\mathbf{L}A^{4+}$	5.0(2)	40.8(3)	−35.8(2)	4.2(3)	33.9(4)	−29.7(3)	0.4(2)	44.3(4)	−43.9(2)
$H_7\mathbf{L}^{7+} + AH^{2-} = H_8\mathbf{L}A^{5+}$	−27.6(2)	8.1(4)	−35.7(2)	0.8(2)	29.3(4)	−28.5(2)	−43.9(2)	0.0(4)	−43.9(2)
$H_8\mathbf{L}^{8+} + AH^{2-} = H_9\mathbf{L}A^{6+}$	−54.4(3)	−21.3(5)	−33.7(3)	−36.8(2)	−10.5(4)	−26.3(2)	−49.4(3)	−6.3(5)	−43.1(3)
$H_8\mathbf{L}^{8+} + AH_2^{-} = H_{10}\mathbf{L}A^{7+}$	−64.7(2)	−33.5(4)	−31.2(2)	−44.3(3)	−20.9(5)	−23.4(3)	−53.5(3)	−9.6(5)	−43.9(3)
$H_8\mathbf{L}^{8+} + AH_3 = H_{11}\mathbf{L}AH^{8+}$	−75.0(3)	−43.5(5)	−29.5(3)	−51.9(3)	−31.4(5)	−20.5(3)	−51.2(2)	−13.3(4(	−37.9(3)
L = L2									
$H_2\mathbf{L}^{2+} + A^{3-} = H_2\mathbf{L}A^{-}$							9.2(3)	33.1(5)	−23.9(3)
$H_3\mathbf{L}^{3+} + A^{3-} = H_3\mathbf{L}A$	−7.5(2)	8.8(4)	−16.3(2)	−2.34(6)	18.7(1)	−21.11(6)	6.7(3)	31.4(6)	−24.7(3)
$H_4\mathbf{L}^{4+} + A^{3-} = H_4\mathbf{L}A^{+}$	−6.2(4)	10.0(7)	−16.2(4)	−1.1(1)	20.2(1)	−21.3(1)	12.1(3)	40.2(6)	−28.1(3)
$H_5\mathbf{L}^{5+} + A^{3-} = H_5\mathbf{L}A^{2+}$	−5.0(3)	12.5(6)	17.5(3)	−0.21(6)	23.07(11)	−23.28(6)	10.8(3)	41.0(6)	−30.2(3)
$H_6\mathbf{L}^{6+} + A^{3-} = H_6\mathbf{L}A^{3+}$	−2.1(3)	18.0(6)	−20.1(3)	1.05(4)	24.72(8)	−23.67(4)	12.2(3)	44.4(6)	−32.2(3)
$H_7\mathbf{L}^{7+} + A^{3-} = H_7\mathbf{L}A^{4+}$	0.0(3)	23.8(6)	−23.8(3)	3.60(6)	31.27(8)	−27.67(6)	2.0(2)	38.0(4)	−36.0(2)
$H_8\mathbf{L}^{8+} + A^{3-} = H_8\mathbf{L}A^{5+}$	−3.8(2)	25.9(4)	−29.7(2)	9.21(4)	40.13(8)	−30.92(4)	−0.2(2)	38.3(3)	−38.5(2)
$H_9\mathbf{L}^{9+} + A^{3-} = H_9\mathbf{L}A^{6+}$	−1.7(2)	29.8(4)	−31.5(2)	22.2(2)	54.7(3)	−32.5(2)	−0.9(3)	38.9(5)	−39.8(3)
$H_{10}\mathbf{L}^{10+} + A^{3-} = H_{10}\mathbf{L}A^{7+}$	0.8(1)	35.0(2)	−34.2(1)	16.7(5)	53.3(8)	−36.6(5)	−0.5(3)	41.8(5)	−42.3(3)
$H_{10}\mathbf{L}^{10+} + AH^{2-} = H_{11}\mathbf{L}A^{8+}$	−48.5(2)	−16.7(3)	−31.8(2)	−17.6(5)	17.2(8)	−34.8(5)	−53.1(2)	−10.0(4)	−43.1(2)
$H_{11}\mathbf{L}^{11+} + AH^{2-} = H_{12}\mathbf{L}A^{9+}$	−25.1(3)	2.5(5)	−27.6(3)	−27.5(5)	3.8(9)	−31.3(6)	−69.4(2)	−28.9(4)	−40.5(2)
$H_{11}\mathbf{L}^{11+} + AH_2^{-} = H_{13}\mathbf{L}A^{10+}$				−33.9(6)	−3.99(11)	−29.9(6)	−69.9(2)	−30.1(4)	−39.8(2)
$H_{11}\mathbf{L}^{11+} + AH_3 = H_{14}\mathbf{L}A^{11+}$				−29.7(6)	−1.8(11)	−27.9(6)	−68.8(3)	−32.2(5)	−36.6(3)

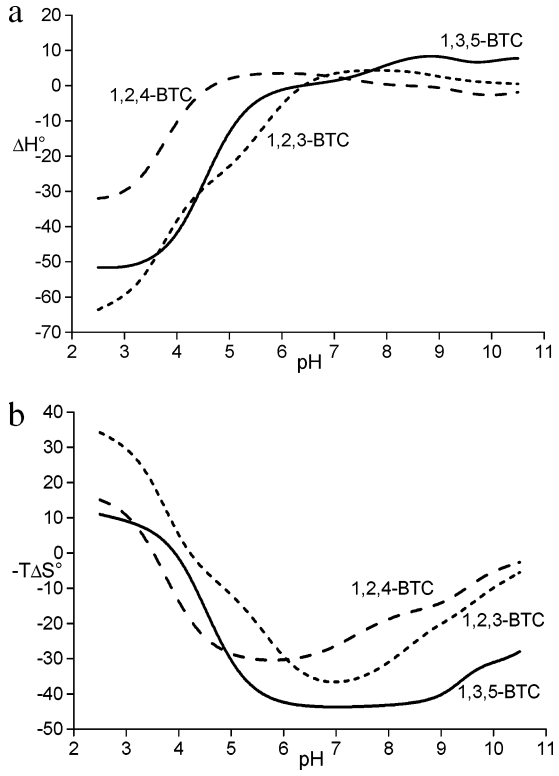

FIGURE 7. pH dependence of the enthalpic (a) and entropic (b) conditional contributions for the complexation of 1,3,5-BTC (solid lines), 1,2,4-BTC (dashed lines), and 1,2,3-BTC (dotted lines) with **L1**.

upon complex formation, electrostatic (from charge−charge to dipole−dipole) interactions, hydrogen bonding. However, it is accepted that charge−charge and hydrogen bond interactions play the mayor role in the stabilization of complexes between charged species, especially in solvents with high dielectric constant such as water.[2,30,31]

The $\Delta H°_{cond}$ and $-T\Delta S°_{cond}$ trends observed in the pH region 11−6 are in accord with the formation of −N−H$^{+}\cdots^{-}$O− contacts. The thermodynamic contributions to ion pairing processes are strongly dependent on the dielectric constant of the medium; in solvents with high dielectric constant, such as water, the ion-pairing process is generally accompanied by largely favorable entropic terms, basically deriving from desolvation of the interacting functions determined by charge neutralization, with consequent increase of translational entropy.[32] At the same time, the favorable enthalpic contribution due to the charge−charge interactions is generally compensated by the unfavorable enthalpic change due to desolvation of the two interacting charged functions.

This result is in accord with the structures derived from MD calculations, which show the formation of NH$^{+}\cdots^{-}$O− interactions in all the system under investigation. Among the different substrates, the highest stability of the 1,3,5-BTC adducts is due to the larger entropic changes, while the enthalpic contributions is more unfavorable ($\Delta H° > 0$) than in the case of the 1,2,3- and 1,2,4-BTC complexes ($\Delta H° \approx 0$), accounting for a the formation of stronger charge−charge interactions and a consequent larger desolvation of the two interacting functions.

Protonation of the BTC trianions at slightly acidic pH values is accompanied by a progressive decrease of

(30) De Robertis, A.; De Stefano, C.; Foti, C.; Giuffrè O.; Sammartano, S. *Talanta* **2001**, 54, 1135−1152.

(31) Conway, B. E. In *Comprehensive Treatise on Electrochemistry*; Bockris, J. O'M., Conway, B. E., Yeager, E., White, R. E., Eds.; Plenum: New York, 1981; Vol. 5.

(32) Bianchi, A., Garcia-España, E. In *Supramolecular Chemistry of Anions*; Bianchi, A., Garcia-España, E., Bowman-James, K., Eds.; Wiley-VCH: New York, 1997; Chapter 6, pp 217−266 and references therein.

$\Delta H°_{cond}$ and increase of $-T\Delta S°_{cond}$, to give an "enthalpy driven" process of complex formation below pH 5−6, as shown in Figure 7a ,b. This behavior is in accord with the formation of an increasing number of hydrogen bonding contacts of the type $-NH^+\cdots OH-$ or $-N\cdots HO-$, generally characterized by a lower or negligible charge neutralization, and consequent lower or negligible desolvation effects. It is known, however, that the contribution of these kinds of interaction to the overall stability of the complexes in aqueous solutions is lower than that of charge−charge $-NH^+\cdots O^-$ interactions. The relatively high stability of the complexes with the protonated forms of the substrates, therefore, suggests the encapsulation of the substrates even in their less charged forms, with a consequent formation of several stabilizing hydrogen bonds contacts.

Experimental Section

General Methods. Receptors **L1** and **L2** were obtained as previously described.[26] ^{1}H NMR spectra were recorded on a 300 MHz spectrometer. In the ^{1}H NMR titrations HCl and NaOH were used to adjust the pH values. The pH was calculated from the measured pD values by using the eqn: pH = pD − 0.40.[33]

Potentiometric Measurements. Receptor and BTC anions protonation constants and equilibrium constants for the complexation reactions were determined by pH-metric measurements (pH = −log [H$^+$]) in 0.1 M NMe_4Cl at 298.1, using the potentiometric equipment already described.[34] The combined glass electrode was calibrated as a hydrogen concentration probe by titrating known amounts of HCl with CO_2-free NMe_4OH solutions and determining the equivalent point by Gran's method,[35] which allows to determine the standard potential $E°$, and the ionic product of water (pK_w = 13.83(1) at 298.1 in 0.1 M NMe_4Cl, K_w = [H$^+$][OH$^-$]). Ligand concentration was 1×10^{-3} M, while substrate concentration varied from 0.5×10^{-3} to 5×10^{-3} M. At least three titration experiments (of about 100 data points each) were performed in the pH range 2.5−11. The computer program HYPERQUAD[36] was used to calculate equilibrium constants from emf data. All titrations were treated either as single sets or as separate entities for each system without significant variation in the values of the determined constants. In the HYPERQUAD program the sum of the weighted square residuals on the observed emf values is minimized. The weights were derived from the estimated errors in emf (0.2 mV) and titrant volume (0.002 cm^3). The most probable chemical model was selected by following a strategy based on the statistical inferences applied to the variance of the residuals, σ^2. The sample standard deviation should be 1, in the absence of systematic errors and when a corrected weighting scheme is used. However, the agreement is considered good for standard deviation values smaller than 3 (σ^2 < 9). Values of σ^2 lower than 6 were obtained for all the refined equilibrium models in the present work. If more than one model gave acceptable σ^2, the reliability of the proposed speciation models was checked by performing F tests at the 0.05 confidence level, using the method reported in ref 37 for two different proposed models, A and B. Assuming that the minimum value of the sample variance, σ_A^2, has been reached for the proposed model A, an alternative model B, which supplies a value of the variance σ_B^2 was rejected if $\sigma_B^2/\sigma_A^2 > F$, where σ_A and σ_B are given directly by data treatment with the HYPERQUAD[36] program. The F values were taken from ref 37. For all the systems investigated, this method leads to define univocally one acceptable system.

Molecular Dynamics Calculations. The theoretical calculations were performed by using the CHARMM force field,[28] as implemented in the Hyperchem 7.51 package.[29]

Different trajectories for molecular dynamics calculations at 1000 K were calculated, 100 ps for free anions and protonated ligands ($[H_7\mathbf{L1}]^{7+}$ and $[H_9\mathbf{L2}]^{9+}$), and 500 ps for all the $[H_n\mathbf{L}A]^{n+}$ adducts (A = BTC trianion). Heating and equilibration (10 ps) were performed before each dynamics simulation. Proton distribution in free protonated ligands and in the complexes was deduced by the NMR data. Atomic charges for receptors and substrates were calculated at the PM3 semiempirical level.[38] To obtain the starting conformations for the $[H_n\mathbf{L}A]^{n+}$ complexes, the lowest energy conformer of each protonated receptor, obtained from MD simulations, was manually docked to the substrate (minimum distance between the atoms of receptor and substrate > 5 Å) and then freely minimized. During the MD trajectories a structure was relaxed through energy minimization at 0 K every 10 ps. The Polak−Ribiere (coniugate gradient) algorithm was used in the minimization procedures to a root-mean-square (RMS) energy gradient less than 0.001 kcal mol^{-1} Å^{-1}. In energy calculation no cutoff distance function was employed for van der Waals terms. A distance-dependent dielectric factor ($\epsilon = 4R_{ij}$) qualitatively simulates the presence of water; the same results were obtained using a constant dielectric factor greater than 1. During the molecular dynamics trajectories calculations, distance restrains (additional force constant = 7 kcal mol^{-1} Å^2) between different atoms of the receptor and of the substrate were attempted to maintain them in close proximity. These restrains were then removed during minimization of final conformations. Analogous calculations have been performed without applying restrains in the gas phase (ϵ = 1), and no significant differences have been observed in the results. The 50 minimized structures from 500 ps dynamic trajectories were clustered in different conformational families on the basis of values of coordinates RMSD (root means square deviation) lower than 1. Each family can be considered as representative of a relevant collection of configurations.

Calorimetric Measurements. The enthalpies of ligand and BTC anion protonation and of anion complexation were determined in 0.1 M NMe_4Cl solution by means of an automated system composed of a thermometric thermal activity monitor equipped with a perfusion-titration device coupled with a 0.250 cm^3 gastight syringe. The measuring vessel was housed in a 25 L water thermostat, which was maintained at the chosen temperature within $\pm 2 \times 10^{-4}$ K. The calorimeter was checked by determining the enthalpy of reaction of strong base (NMe_4OH) with strong acid (HCl) solutions. The value obtained, −13.55(5) kcal mol^{-1}, was in agreement with the literature values.[39] Further checks were performed by determining the enthalpies of protonation of ethylendiamine.

In a typical experiment, an NMe_4OH solution (0.1 M, addition volumes 15.00 ± 0.03 μL) was added to acidic solutions of the ligands (5×10^{-3} M, 1.2 cm^3) containing equimolar quantities of the anion in the complexation experiments. Corrections for the heats of dilution were applied. At least three titrations (about 120 data points) were performed for each system. The titration curves for each system were treated either as a single set or as separated entities without significant variation in the values of the enthalpy changes. Further measurements were performed by adding anion solutions to ligand solutions in order to get independent confirmations of the enthalpy changes obtained for specific

(33) Covington, A. K.; Paabo, M.; Robinson, R. A.; Bates, R. G. *Anal. Chem.* **1968**, *40*, 700−710
(34) Bianchi, A.; Bologni, L.; Dapporto, P.; Micheloni, M.; Paoletti, P. *Inorg. Chem.* **1984**, *23*, 1201−1205.
(35) (a) Gran, G. *Analyst* (*London*) **1952**, *77*, 661−663. (b) Rossotti, F. J.; Rossotti, H. *J. Chem. Educ.* **1965**, *42*, 375−378.
(36) Gans, P.; Sabatini, A.; Vacca, A. *Talanta* **1996**, *43*, 807−812.
(37) Hamilton, W. C. *Statistics in Phisycal Chemistry*; The Ronald Press Co.: New York, 1964.
(38) Stewart, J. P. P. *J. Comput.-Aided Mol. Des.* **1990**, *4*, 1−105
(39) Smith, R. M.; Martell, A. E. NIST Critical Stability Constants Database, version 2, 1995.

complexed species. Independent measurements were performed to determine ligand protonation and complexation enthalpy changes.

Under the reaction conditions and employing the determined protonation constant, the concentrations of the species present in solution before and after addition were calculated and the corresponding enthalpies of reaction were determined from the calorimetric data by means of the AAAL program.[40]

Acknowledgment. Financial support by the Italian Ministero dell'Università e della Ricerca Scientifica e Tecnologica (COFIN 2002) is gratefully acknowledged.

Supporting Information Available: ORTEP drawings for $[(Na(ClO_4)_6)\subset \mathbf{L1}_2H_{13}]^{8+}$. Plot of the chemical shifts of the **L2** ^{1}H NMR signals as a function of pH, distribution diagrams for the systems 1,2,3-BTC/**L** and 1,2,4-BTC/**L** (**L** = **L1** or **L2**), and plots of the chemical shifts of the ^{1}H NMR signals of the BTC isomers in the presence of increasing amount of **L1** or **L2**. Cartesian coordinates, atomic charges, and atom types for the lowest energy conformers for the BTC trianions $[H_7\mathbf{L1}]^{7+}$, $[H_9\mathbf{L1}]^{9+}$, and their complexes. Description of the lowest energy conformers of the $[H_7\mathbf{L1}A]^{4+}$ complexes with different disposition of the brigehead nitrogen. Description of the lowest energy conformers of the $[H_9\mathbf{L1}A]^{6+}$ complexes. Lists of the hydrogen-bond contacts for the lowest energy conformers of the $[H_7\mathbf{L1}A]^{4+}$ and $[H_9\mathbf{L1}A]^{6+}$ complexes (A = 1,2,3-BTC, 1,2,4-BTC, or 1,3,5-BTC). Thermodynamics parameters for protonation of **L1**, **L2**, and BTC isomers. pH dependence of enthalpic and entropic conditional changes for the complexes with **L2**. This material is available free of charge via the Internet at http://pubs.acs.org.

JO048142P

(40) Vacca, A. AAAL program, Department of Chemistry, University of Florence, Florence, 1997.